

Phase referencing and narrow-angle astrometry in current and future interferometers

Benjamin F. Lane^a and Matthew W. Muterspaugh^a

^aMIT Center for Space Research, 70 Vassar St., Cambridge, MA. 02139, USA;

Copyright 2004 Society of Photo-Optical Instrumentation Engineers.

This paper will be published in SPIE conference proceedings volume 5491, "New Frontiers in Stellar Interferometry," and is made available as an electronic preprint with permission of SPIE. One print or electronic copy may be made for personal use only. Systematic or multiple reproduction, distribution to multiple locations via electronic or other means, duplication of any material in this paper for a fee or for commercial purposes, or modification of the content of the paper are prohibited.

ABSTRACT

Atmospheric turbulence is a serious problem for ground-based interferometers. It places tight limits on both sensitivity and measurement precision. Phase referencing is a method to overcome these limitations via the use of a bright reference star. The Palomar Testbed Interferometer was designed to use phase referencing and so can provide a pair of phase-stabilized starlight beams to a second (science) beam combiner. We have used this capability for several interesting studies, including very narrow angle astrometry. For close (1-arcsecond) pairs of stars we are able to achieve a differential astrometric precision in the range 20–30 micro-arcseconds.

Keywords: Optical/IR Interferometry, Phase referencing, Astrometry

1. INTRODUCTION

Although they provide very high angular resolution, ground-based stellar interferometers suffer from very limited sensitivity. This is a consequence of atmospheric turbulence which corrupts the incoming stellar wavefront on very short timescales and over small distances. Typical numbers for atmospheric coherence length and time are $r_0 = 10\text{cm}$ and $\tau_0 = 2\text{ms}$ at visible wavelengths. An interferometer must collect enough photons in a coherence volume ($\sim r_0^2 \tau_0$) to detect fringes. Optimistically assuming a system throughput of 10%, this would place the S/N=3 tracking limit at $\sim 8\text{th}$ magnitude, assuming no detector noise.

There are several ways to overcome this sensitivity limit. The most obvious – and most expensive – is to put the interferometer in space,¹ or at least at some location with favorable atmospheric properties such as Antarctica.² It is also crucial to maximize system throughput and reduce other noise sources such as detector read-noise.³ It should also be noted that both r_0 and τ_0 scale approximately as $\lambda^{6/5}$ and thus going to longer wavelengths will rapidly improve the situation. This is why the current generation of interferometers often work in the near-IR.

In recent years, much work has been done to increase the apparent r_0 via the use of adaptive optics⁴ (AO); this has been successful at both the Keck Interferometer⁵ and the VLTI.⁶ The use of AO-corrected apertures provides a substantial improvement in collecting power, i.e. by a factor of $\sim S \times (D/r_0)^2$, where S is the AO Strehl ratio and D is the size of the AO-corrected aperture. For a large aperture and a typical AO Strehl one might expect an improvement by a factor of 100–300, as long as a natural or laser guide star is available.

However, it is not clear that such an improvement will be sufficient for certain areas of research, e.g. for imaging faint extra-galactic objects or for narrow-angle astrometry.⁷ An additional approach is to find a way to increase the effective atmospheric coherence time, τ_0 . This can be done by simultaneously observing a bright reference star and the science target using two separate interferometric beam-combiners, and using the reference

Further author information: (Send correspondence to B.F.L.)

B.F.L.: E-mail: blane@mit.edu, Telephone: 1 617 253-3429

M.W.M: E-mail: matthew1@mit.edu, Telephone: 1 617 547-1758

star to determine the fringe motion introduced by the atmosphere. This is known as phase referencing. By using a sufficiently fast control loop (~ 100 Hz) it is possible to remove much of the fringe motion in real time, and hence provide an artificially long coherence time for the beam combiner used to observe the science target. In principle one could consider extending the maximum allowed integration time from milliseconds to seconds or even minutes, with a corresponding increase in sensitivity. Of course, it should be noted that phase referencing, like AO, requires a bright reference.

In this paper we discuss recent progress in the area of phase referencing⁸ as applied to very narrow-angle differential astrometry.⁹ In particular, we have used the Palomar Testbed Interferometer in a phase-referencing mode that allows us to achieve very high precision relative astrometry between 0.1-arcsecond pairs of stars; such astrometry would be useful in searching for planets orbiting one of the components in the system. This instrumental configuration can also be used to obtain simultaneous high spectral and spatial resolution data through the use of double-Fourier interferometry.¹⁰

The Palomar Testbed Interferometer¹¹ (PTI) is a long-baseline infrared interferometer located at Palomar Observatory near San Diego, California. It typically operates in the H ($1.6\mu\text{m}$) and K ($2.2\mu\text{m}$) bands. It has three 40-cm diameter apertures separated by 110-m and 80-m baselines, giving a maximum angular resolution of ~ 3 milli-arcseconds.

2. PHASE REFERENCING

Atmospheric turbulence above the interferometer can be characterized by a distance over which the wavefront remains flat. This distance is known the atmospheric coherence length. For typical observing sites, we have

$$r_0 \simeq 0.1 \left(\frac{\lambda}{0.5\mu\text{m}} \right)^{6/5} \text{ m} \quad (1)$$

In addition, since the atmosphere is not static, the wavefront errors change on timescales of $\tau_0 \sim r_0/v$ where v is a wind speed. The resulting phase perturbations obey an $f^{-8/3}$ power law. An example of measured fringe motion is given in Figure 1. The fringe motion will tend to “smear” the fringe, reducing fringe visibility and hence signal-to-noise ratio.

The phase fluctuations introduced by the atmosphere are correlated over small angles, characterized by the angular isoplanatic angle θ_0 such that

$$\langle \sigma_\theta^2 \rangle = \left(\frac{\theta}{\theta_0} \right)^{5/3} \quad (2)$$

where

$$\theta_0 = \left[2.914k^2(\sec \phi)^{8/3} \int C_n^2(z) z^{5/3} dz \right]^{-3/5} \quad (3)$$

C_n^2 is a parameter representing the turbulence amplitude, $k = 2\pi/\lambda$ is the wavenumber of the light and ϕ is the zenith angle of the observation.

If one has available an estimate of the fringe motion induced by the atmosphere, it is sometimes possible to correct the phase and recover the fringe signal. If the fringe is detected using an integrating detector, or a detector with a non-zero read-noise, it is necessary to apply the phase correction in real-time, i.e. by rapidly adjusting the instrumental delay using a fast delay line or similar device. The phase reference can be obtained in many different ways; it can be provided by a nearby reference star (located within the isoplanatic patch, ~ 30 arcseconds in the near-IR), or it can be the science target itself, observed at a different wavelength or with a different beam-combiner (which may be optimized for phase measurement). It may even be possible to provide a phase reference by measuring some fraction of the atmospheric pathlength changes using a laser.¹² In any case, the phase referencing system needs a fast control loop to sense and correct the atmospheric pathlength errors on millisecond timescales. The effect of atmospheric turbulence, with and without active phase referencing is shown in Figure 2.

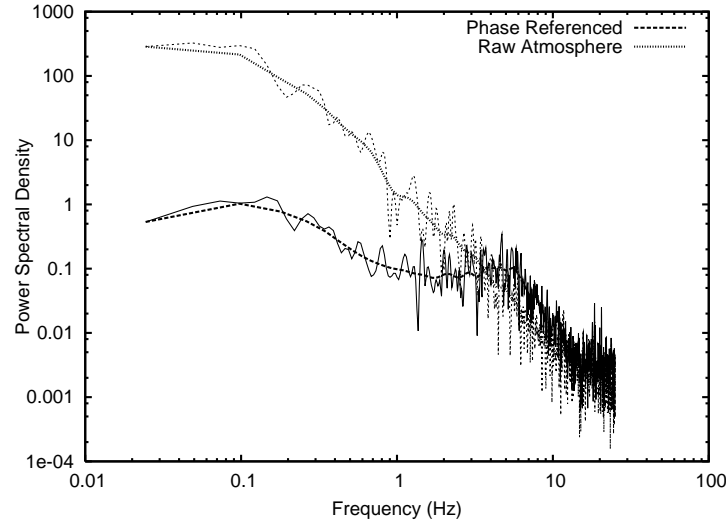


Figure 1. Power spectral density of the measured fringe phase, obtained using a fringe tracker at PTI, with and without phase referencing. The atmosphere induces fringe motion that has a power-law dependence ($P(f) \propto f^{-8/3}$)

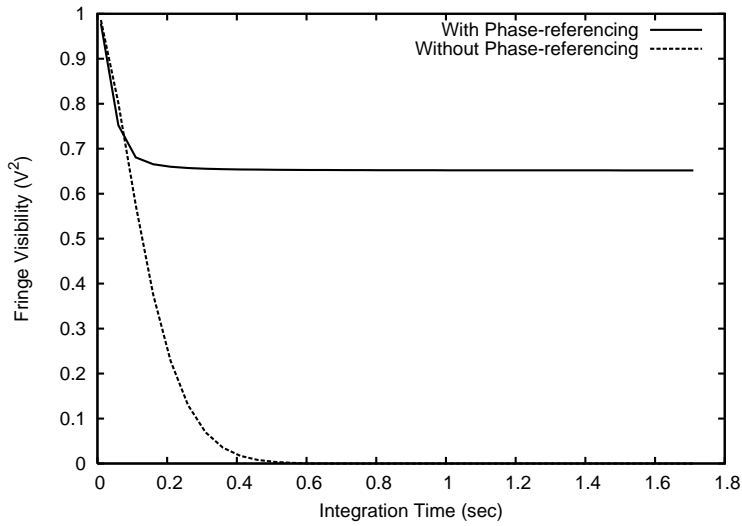


Figure 2. The effect of integration time on measured fringe visibility, with and without phase referencing. Model parameters were appropriate for PTI, with a fringe tracker update rate of 100 Hz. On timescales shorter than the fringe-tracker closed-loop bandwidth, phase referencing has little effect. However, it does remove the fringe motion at low frequencies, which would – if left uncorrected – completely wash out the fringe.

Clearly, phase referencing opens up a new regime for interferometry, as beam-combination instruments can begin to work with exposure times measured in seconds. This will allow the use of instruments that are not necessarily optimized for short-exposure phase measurements but rather high spectral resolution or high-precision visibility measurements. This capability may also be applicable to multi-aperture combination,¹³ in that for an N -aperture interferometer it is only necessary to fringe-track on N baselines in order to keep the array “phased”. The full set of $N(N-1)/2$ baselines can then be combined in a different, dedicated beam-combiner.

3. ASTROMETRY

One application that can take advantage of phase referencing is narrow-angle astrometry. In this case one is interested in measuring the angle between a close pair of stars to very high precision; such astrometry can be used both to determine orbital parameters (which can be combined with radial velocity and photometry data to determine component masses, distances and luminosities) to high precision, and to search for planets in the system.

PTI is unique among current interferometers in that it has a “dual-star” configuration, which makes it possible to simultaneously track two close (separation ≤ 60 arcseconds) stars. To achieve this, PTI is equipped with two separate optical trains and beam-combiners that share the same apertures. PTI is also particularly suited to phase-referencing in that it is capable of fringe-tracking at bandwidths high enough to follow atmospheric motion, and hence one beam combiner can track and correct the atmosphere while the other can be used for high-precision measurements.

For close pairs of stars, astrometric errors introduced by the atmosphere will tend to be common-mode, and hence will subtract out of a differential measurement. Shao & Colavita⁷ quantified this effect (in arcseconds of astrometric error) as

$$\sigma_a = 540B^{-2/3}\theta t^{-1/2} \quad (4)$$

where B is the baseline in meters, θ is the angular separation (in radians) of the stars, and t the integration time in seconds.

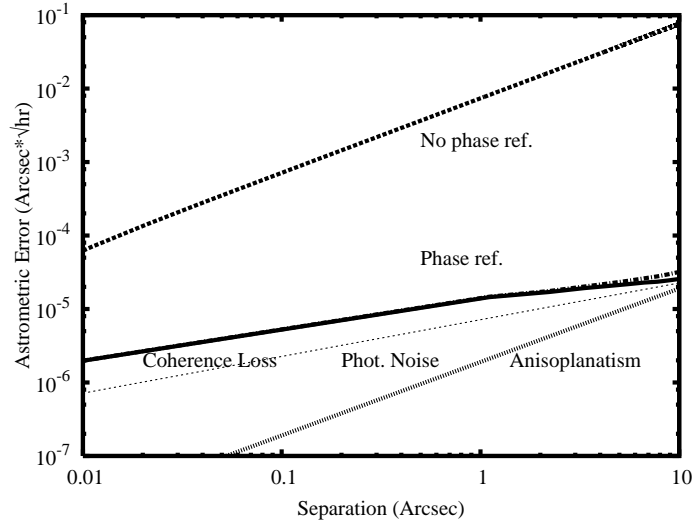


Figure 3. The expected narrow-angle astrometric performance in arcseconds for the phase-referenced fringe-scanning approach, for a fixed scan rate. There are three primary sources of astrometric error in this method: angular anisoplanatism,⁷ temporal decoherence,⁸ and photon noise. Also shown is the magnitude of the temporal decoherence effect in the absence of phase referencing, illustrating why stabilizing the fringe via phase referencing is necessary.

From Equation 4 it is clear that at small separations the atmospheric error becomes negligible. This motivated us to modify PTI so as to allow us to study binaries with separations on the order of 0.1–1 arcseconds, i.e. larger

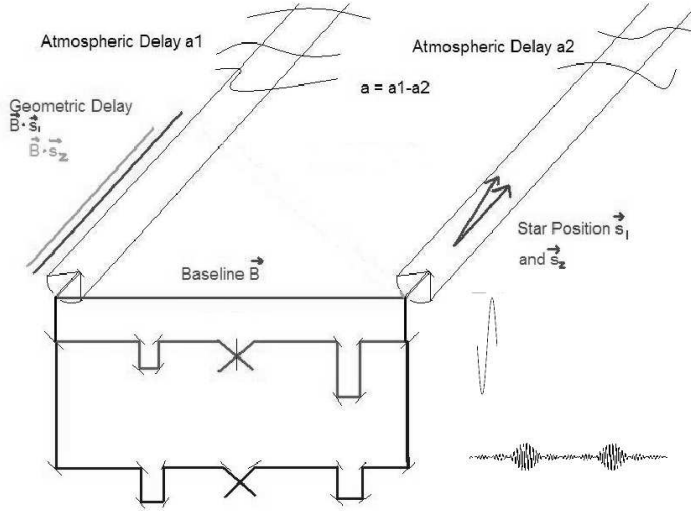


Figure 4. The instrument configuration for phase-referenced narrow-angle astrometry. One beam-combiner is used to track and correct for atmospheric turbulence; corrections it derives are applied to both delay lines. The second beam combiner scans over $\sim 200\mu\text{m}$ in differential optical path, tracing out the double-fringe packet produced by a close binary star.

than the nominal interferometric field of view (given by $\lambda/\Delta\lambda \times \lambda/B$), but smaller than the 30–60 arcseconds previously considered for narrow-angle astrometry.⁷ The probability of finding a background reference star in this reduced field is very small, but outweighed by the fact that binary stellar systems with these apparent separations are quite common.

For a binary separation of 0.1 arcsecond and an interferometric baseline of 100 meters, the predicted error due to the atmosphere is $\sim 0.2\mu\text{arcsecond}$ in an hour. Of course, there are additional sources of astrometric error, including photon noise and potential systematic errors associated with the instrument. In particular, if the measurements of the two stars are not truly simultaneous – as in this case, see below – there will be a small error associated with fringe motion during the time between the measurements. Nevertheless, we estimate that PTI should be able to obtain an astrometric precision at the level of $10\mu\text{arcseconds}$ in an hour of observation (Figure 3).

3.1. Instrument Configuration

We configured PTI to observe close (separation less than 1 arcsecond) visual binaries, so-called “speckle binaries”. In this configuration (Figure 4), the incoming starlight was split 70/30 between a fringe tracker running at 100 Hz and a second, astrometric beam combiner. The astrometric beam combiner did not track the fringe but rather it measured the intensity of the combined stellar beams while the relative optical path between the arms of the interferometer was modulated (using a differential delay line) in a triangle-wave pattern with an amplitude of $\sim 100\mu\text{m}$ and a period of $\sim 1\text{Hz}$. An example of this data is given in Figure 5.

3.2. Data Processing

We extract the relative astrometric positions from data such as that shown in Figure 5 as follows. First, we construct a search grid in differential R.A. and declination over which to search. For each point in the search grid we calculate the expected differential delay based on the interferometer location, baseline geometry, and time of observation for each scan. A model of a double-fringe packet is then calculated and compared to the observed scan to derive a χ^2 value; this is repeated for each scan, co-adding all of the χ^2 values associated with that point in the search grid. The final χ^2 surface as a function of differential R.A. and declination is thus derived. The best-fit astrometric position is found at the minimum- χ^2 position, with uncertainties defined by

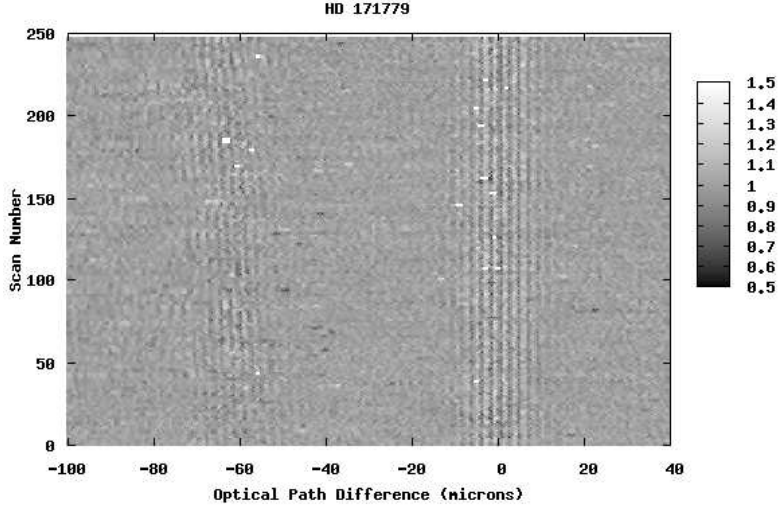


Figure 5. Measured intensity in the detector as a function of differential optical path, for successive scans of the speckle binary system HD 171779. Each scan takes 1.5 seconds to acquire. The fringe tracker was locked on to the bright star (around 0), while the second star produces a fringe pattern which starts at $-60 \mu\text{m}$ and moves due to baseline rotation. Although the second fringe pattern is relatively faint, the effect of co-adding 500–2000 scans produces a high signal-to-noise ratio in the final astrometric measurement.

the appropriate χ^2 contour – which depends on the number of degrees of freedom in the problem and the value of the χ^2 -minimum. Because the data was obtained with a single-baseline instrument, the resulting error contours are very elliptical, with aspect ratios at times ≥ 10 .

One potential complication with fitting a fringe to the data is that there are many local minima spaced at multiples of the operating wavelength. If one were to fit a fringe model to each scan separately and average (or fit an astrometric model to) the resulting delays, one would be severely limited by this fringe ambiguity (for a 110-m baseline interferometer operating at $2.2\mu\text{m}$, the resulting positional ambiguity is ~ 4.6 milli-arcseconds). However, by using the χ^2 -surface approach, and co-adding the probabilities associated with all possible delays for each scan, the ambiguity disappears. This is due to two things, the first being that co-adding simply improves the signal-to-noise ratio. Second, since the observations usually last for an hour or even longer, the associated baseline change due to Earth rotation also has the effect of “smearing” out all but the true global minimum. The final χ^2 -surface does have dips separated by ~ 4.6 milli-arcseconds from the true location, but they only show up at the 40σ contour level.

3.3. Preliminary Results

We have obtained exploratory data on 25 binaries, and have intensively followed the binary system HD 171779 in order to evaluate the performance and repeatability of our system (Figure 6). HD 171779 is a pair of K-giants in a long-period orbit, such that the apparent motion is nearly linear over the few months of observation. A typical observation of this pair takes an hour, and produces a formal 1σ error ellipse approximately $5 \times 100 \mu\text{-arcseconds}$ in size; the smaller axis being aligned with the mean baseline orientation (which in turn depends on the exact timing of the observation). A linear two-dimensional (taking into account the full shape of the error ellipse) fit of 15 nights of data produces a reduced $\sqrt{\chi^2_r} = 4.7$, indicating that the formal errors underestimate the true errors by a factor of 4.7. We note that fits to 1-D projections (e.g. along the declination or R.A. axis) show similar values of reduced χ^2 , indicating that the error scaling is uniform. Hence we conclude that the night-to-night repeatability is 24 and $470 \mu\text{-arcseconds}$ in the minor and major axes respectively. We note that we have recently improved aspects of the instrument metrology system and data processing, and expect to achieve the $10 \mu\text{-arcsecond}$ goal in the next few months.

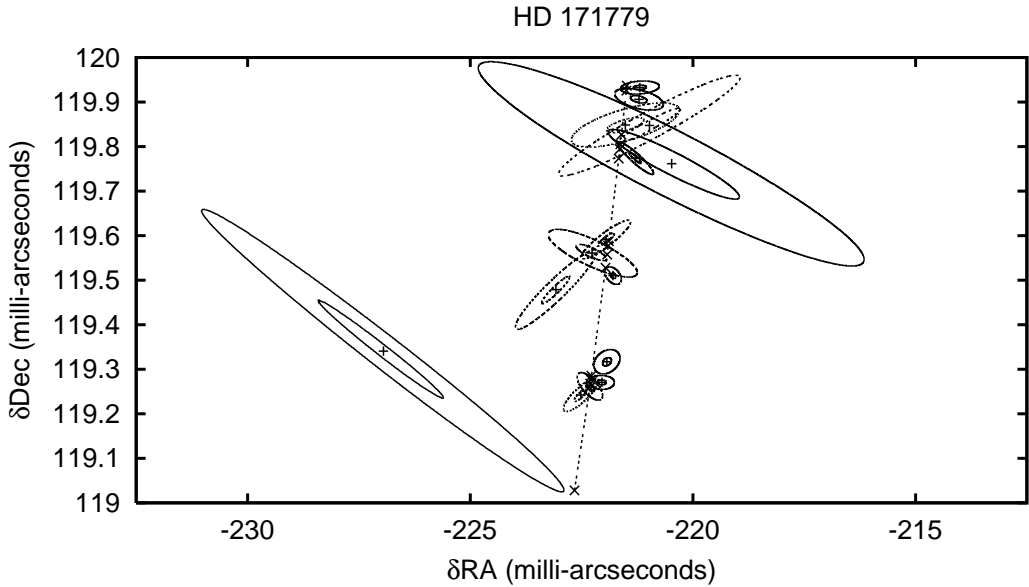


Figure 6. Measured differential astrometry between the components of the speckle binary HD 171779, together with a best-fit orbital motion curve. The contours represent the formal $1-\sigma$ and $4-\sigma$ uncertainties. Note that the single-baseline configuration used to obtain this data is sensitive primarily in the declination direction, and therefore the Declination-axis has been magnified by a factor of 10 compared to the R.A. axis. This data implies a night-to-night astrometric repeatability of $24 \mu\text{-arcseconds}$ in the direction of greatest sensitivity (approximately aligned to the declination axis), and a somewhat less impressive $470 \mu\text{-arcsecond}$ repeatability in the orthogonal direction.

4. DISCUSSION

Ground-based interferometers are severely challenged by the effects of atmospheric turbulence. The short integration times required in the absence of any active compensation limits interferometry to all but the brightest astronomical sources, and limits the types of observations that can be done (spectral resolution, multi-aperture combination etc). One solution is to divide the problem into two parts which can be optimized separately. A phase-tracking beam-combiner can use either a nearby reference source or the science target itself – if it is sufficiently bright – to stabilize the phase of the incoming stellar wavefront. A second, science-optimized beam combiner can then obtain desired data at a relatively leisurely pace.

We have used a phase-referencing approach to observe close pairs of binaries (separations less than 1 arc-second) in order to obtain very high precision differential astrometry. Over 15 nights of data on the binary HD 171779 we find a night-to-night repeatability of approximately $24 \mu\text{-arcseconds}$ in one axis. This level of astrometric precision is sufficient to begin a search for Jupiter-mass planets around the components of nearby binary stellar systems, given that simulations¹⁴ indicate there are regions where planets can persist indefinitely (i.e. sufficiently close to one of the stellar components). A dedicated astrometric survey could quickly answer the question of whether or not planets form in these comparatively close systems. We have begun such a survey, PHASES (“Palomar High-precision ASTrometric Exoplanet Search”) and hope to have results in the next few years.

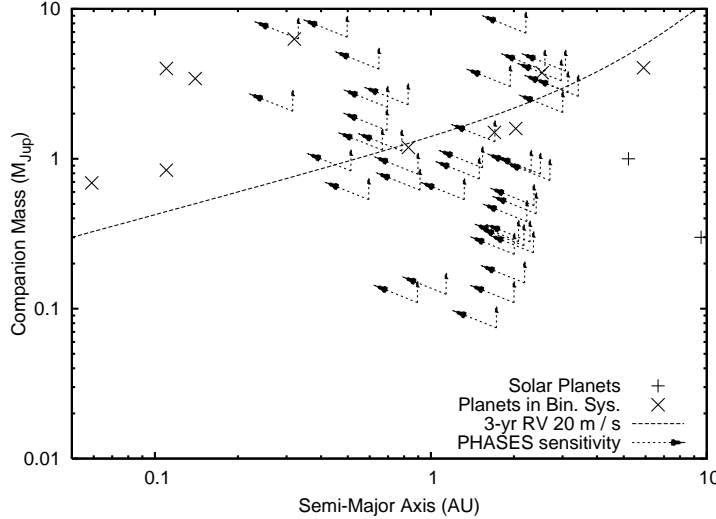


Figure 7. Phase space explored by radial velocity and astrometry. The figure shows the areas in the semi-major axis vs. companion mass plane explored by a notional astrometry project (“PHASES”), for each specific target in our sample; astrometry will find any planet located above and to the left of the arrows. This accounts for the actual mass and distance to the binaries in question. Also shown are a number of planets known to exist in wide (2 arcsec separation) binary systems. The precision for the RV sample is 20 m s^{-1} which is a realistic value given the additional photon noise and systematics present for compact binaries. For binary separations of 10 AU, companions in orbits inside approximately 1 AU are expected to be stable; the stability zone grows with increasing binary separation.

ACKNOWLEDGMENTS

It is a pleasure to thank M. Colavita, S. R. Kulkarni, B. F. Burke, M. Konacki, A. Boden, N. Safizadeh and K. Rykoski for their contributions to the astrometry effort. Observations with PTI are made possible through the efforts of the PTI Collaboration, which we acknowledge. Interferometer data was obtained at the Palomar Observatory using the NASA Palomar Testbed Interferometer, supported by NASA contracts to the Jet Propulsion Laboratory. This research has made use of the Simbad database, operated at CDS, Strasbourg, France. MWM acknowledges the support of the Michelson Graduate Fellowship program. BFL gratefully acknowledges support from a Pappalardo Fellowship in Physics.

REFERENCES

1. S. C. Unwin and M. Shao, “Space Interferometry Mission,” in *Proc. SPIE Vol. 4006, p. 754-761, Interferometry in Optical Astronomy, Pierre J. Lena; Andreas Quirrenbach; Eds.*, pp. 754–761, July 2000.
2. J. P. Lloyd, B. R. Oppenheimer, and J. R. Graham, “The Potential of Differential Astrometric Interferometry from the High Antarctic Plateau,” *Publications of the Astronomical Society of Australia* **19**, pp. 318–322, 2002.
3. A. G. Basden and C. A. Haniff, “Low light level CCDs and visibility parameter estimation,” *MNRAS* **347**, pp. 1187–1197, Feb. 2004.
4. S. K. Saha, “Modern optical astronomy: technology and impact of interferometry,” *Reviews of Modern Physics* **74**, pp. 551–600, Apr. 2002.
5. M. M. Colavita and P. L. Wizinowich, “Keck Interferometer update,” in *Interferometry for Optical Astronomy II. Edited by Wesley A. Traub. Proceedings of the SPIE, Volume 4838*, pp. 79-88 (2003)., pp. 79–88, Feb. 2003.
6. M. Wittkowski, P. Kervella, R. Arsenault, F. Paresce, T. Beckert, and G. Weigelt, “VLTI/VINCI observations of the nucleus of NGC 1068 using the adaptive optics system MACAO,” *A&A* **418**, pp. L39–L42, Apr. 2004.

7. M. Shao and M. M. Colavita, "Potential of long-baseline infrared interferometry for narrow-angle astrometry," *A&A* **262**, pp. 353–358, Aug. 1992.
8. B. F. Lane and M. M. Colavita, "Phase-referenced Stellar Interferometry at the Palomar Testbed Interferometer," *AJ* **125**, pp. 1623–1628, Mar. 2003.
9. B. F. Lane and M. W. Mutterspaugh, "Differential Astrometry of Subarcsecond Scale Binaries at the Palomar Testbed Interferometer," *ApJ* **601**, pp. 1129–1135, Feb. 2004.
10. J.-M. Mariotti and S. T. Ridgway, "Double Fourier spatio-spectral interferometry - Combining high spectral and high spatial resolution in the near infrared," *A&A* **195**, pp. 350–363, Apr. 1988.
11. M. M. Colavita, J. K. Wallace, B. E. Hines, Y. Gursel, F. Malbet, D. L. Palmer, X. P. Pan, M. Shao, J. W. Yu, A. F. Boden, P. J. Dumont, J. Gubler, C. D. Koresko, S. R. Kulkarni, B. F. Lane, D. W. Molley, and G. T. van Belle, "The Palomar Testbed Interferometer," *ApJ* **510**, pp. 505–521, Jan. 1999.
12. C. H. Townes, "The Potential for Atmospheric Path Length Compensation in Stellar Interferometry," *ApJ* **565**, pp. 1376–1380, Feb. 2002.
13. D. Mozurkewich, "Interferometer Design for Synthesis Imaging," in *Principles of Long Baseline Stellar Interferometry*, pp. 231–+, 2000.
14. M. J. Holman and P. A. Wiegert, "Long-Term Stability of Planets in Binary Systems," *AJ* **117**, pp. 621–628, Jan. 1999.